ACS OMEGA

http://pubs.acs.org/journal/acsodf

Article

# Valorizing Plastic-Contaminated Waste Streams through the Catalytic Hydrothermal Processing of Polypropylene with Lignocellulose

Sukanya Hongthong, Hannah S. Leese, and Christopher J. Chuck*

Cite This: *ACS Omega* 2020, 5, 20586−20598

Read Online

ACCESS | Metrics & More | Article Recommendations | Supporting Information

**ABSTRACT:** Food waste is a promising resource for the production of fuels and chemicals. However, increasing plastic contamination has a large impact on the efficiency of conversion for the more established biological routes such as anaerobic digestion or fermentation. Here, we assessed a novel route through the hydrothermal liquefaction (HTL) of a model waste (pistachio hulls) and polypropylene (PP). Pure pistachio hulls gave a biocrude yield of 34% (w/w), though this reduced to 16% (w/w) on the addition of 50% PP in the mixture. The crude composition was a complex blend of phenolics, alkanes, carboxylic acids, and other oxygenates, which did not change substantially on the addition of PP. Pure PP does not breakdown at all under HTL conditions (350 °C, 15% solids loading), and even with biomass, there is only a small synergistic effect resulting in a conversion of 19% PP. This conversion was enhanced through using typical HTL catalysts including Fe, $FeSO_4{\cdot}7H_2O$, $MgSO_4{\cdot}H_2O$, $ZnSO_4{\cdot}7H_2O$, ZSM-5, aluminosilicate, Y-zeolite, and $Na_2CO_3$; the conversion of PP reached a maximum of 38% with the aluminosilicate, for example. However, the PP almost exclusively broke down into a solid-phase product, with no enhancement of the biocrude fraction. The mechanism was explored, and with the addition of the radical scavenger butylated hydroxytoluene (BHT), the conversion of plastic reduced substantially, demonstrating that radical formation is necessary. As a result, the plastic conversion was enhanced to over 50% through the addition of the co-solvent and hydrogen donor, formic acid, and the radical donor, hydrogen peroxide. The addition of formic acid also changed the crude composition, including more carboxylic acids and oxygenated species than the conversion of the biomass alone; however, the majority of the carbon distributed to the volatile organic gas fraction producing an array of short-chain volatile hydrocarbons, which potentially could be repolymerized as a polyolefin or combined with the biocrude for further processing. Catalytic HTL was therefore shown to be a promising method for the valorization of polyolefins with biomass under typical HTL conditions.




## 1. INTRODUCTION

Declining fossil fuel reserves and an increasing awareness of their environmental impact have led to an increased interest in developing alternative resources for energy production. Organic solid wastes such as municipal and agricultural food wastes have huge potential as a renewable energy feedstock and are now starting to be collected and converted into energy such as methane through anaerobic digestion. However, increasing levels of plastic in these waste streams interfere with the biological processing.[1] These plastics are typically polyolefins derived from plastic films and as such have a relatively high energy content; therefore, the valorization of both streams simultaneously is a promising alternative for waste management.

Using pyrolysis, typically at 500 °C, to co-process lignocellulosic and plastics has gained much attention in the last few decades.[2] Under these conditions, polyolefins break down into a range of volatile components, which make it an effective co-material for improving the quality of biomass during co-processing.[3] Polyolefin polymers such as polyethylene and polypropylene (PP) are composed of approximately 14 wt % hydrogen, which make them a good source of liquid hydrocarbons in the process,[4] and therefore when decomposed with biomass through rapid heat processing, the quantity and quality of bio-oil produced can be improved. There have been several studies on co-pyrolysis of plastic and biomass, which showed the beneficial synergistic effects in terms of increased liquid oil conversion.[5]

While pyrolysis offers an effective route to convert the plastic, the waste stream must be dried prior to conversion often reducing the energy balance substantially.[6] This is particularly true of wet feedstock's such as food wastes. A more effective route for processing wet food wastes is through

**Received:** June 15, 2020
**Accepted:** July 23, 2020
**Published:** August 7, 2020







https://dx.doi.org/10.1021/acsomega.0c02854
*ACS Omega* 2020, 5, 20586−20598

hydrothermal liquefaction (HTL), where the slurry is processed between 270 and 350 °C, keeping the water in the liquid phase under pressure, resulting in a biocrude, aqueous phase, and solid residue. The high pressure maintains the solvent in the liquid state and the combination of high pressure and temperature leads to a reduction of the dielectric constant and density, which allows solubility of more non-polar hydrocarbons.[7] Additionally, the key to HTL is the reduction in oxygen content in the bio-crude, which is removed as carbon dioxide and water,[8] leading to lower oxygen content and higher energy liquid crude oil. This makes it more comparable to the heating value for conventional petroleum fuels[9,10] and reduces the operative costs of handling equipment and storage.[11]

While polyolefin/biomass co-liquefaction has been demonstrated under supercritical conditions with temperatures up to 440 °C, above the decomposition temperature of these polymers, this is far beyond the HTL region.[12] There have been far fewer studies into the co-liquefaction of plastic waste blended with biomass in the HTL range, though this could make the reaction conditions milder, allow an improved energy balance through not drying the feedstock, and improve the decomposition of plastic at lower temperatures.[13−15]

The majority of these studies to date have demonstrated the co-liquefaction of plastics with marine algae. The investigation into the co-liquefaction of microalgae and macroalgae with plastic blends, for example, suggested that the presence of plastics can alter the composition of the biocrude fraction and presented some evidence of the minor deposition of the polyolefins in the crude fraction.[16−18] Recently Hongthong et al. demonstrated that a range of plastics could be co-processed with pistachio hulls through hydrothermal liquefaction, with nylon and poly(ethylene terephthalate) (PET) breaking down substantially. However, the polyolefins only demonstrated a minor synergistic effect with less than 7% of the polypropylene and polyethylene being converted under HTL conditions when 20% polymer was added.[19] A similar result was seen for the co-liquefaction with macroalgae.[17]

In the hydrothermal liquefaction process, the presence of catalysts can restrain the side reactions, reduce the operational conditions, increase the chemical reactivity, reduce the formation of solid residues, and enhance the yield and quality of the biocrude.[20] Homogeneous alkali catalysts have been used widely in several investigations. For example, it was reported that alkali catalysts can improve biomass conversion giving a crude with less oxygen and a higher hydrogen content.[21,22] $Na_2CO_3$ is the most frequently used homogeneous catalyst in this regard.[23] Microporous and mesoporous catalysts for the conversion of plastic waste into liquid oil and char have also been reported in several studies recently. Metal catalysts have also gained attention as alternative catalyst support materials due to their high surface area and high chemical stability. Though it should be noted that the HTL conditions of high temperature in an aqueous environment severely limit the use of more unstable organometallic species. A number of groups have demonstrated that the addition of iron (Fe) enhanced the hydrocarbon content and overall yield and quality of the biocrude.[24,25]

The most widely used cracking catalysts are acidic materials such as aluminosilicates and zeolites. Zeolite catalysts are one of the most effective catalysts because they can remove a significant number of oxygenated compounds and have a significant shape-selective effect on the production of aromatics.[26,27] At high temperatures, above 450 °C, during hydrocarbon cracking, the primary vapors diffuse into internal pores of the catalysts, which are absorbed on the acid sites and converted to hydrocarbons.[28] Indeed in the HTL reaction, a zeolite catalyst was demonstrated to increase biocrude yields in the liquefaction of *Nannochloropsis*.[29]

Formic acid (FA) is also a widely used catalyst in liquefaction. Formic acid is one of the main products from biomass decomposition and is attractive as both an organic catalyst and as a sustainable source of hydrogen as it can break down into $H_2$ and $CO_2$.[30] When used under HTL conditions, the formic acid is thought to act as an acid catalyst, promoting hydrolysis of the biopolymers at lower temperatures, increasing the interaction of soluble products, and is a source of $H_2$ as the acid can degrade over heterogeneous catalysts to produce hydrogen. Interestingly, formic acid has been demonstrated to give higher bio-oil yields, in the liquefaction of lignin, than the liquefaction with hydrogen gas. The authors reasoned that the hydrogen was being released in the liquid phase, as such formic acid was able to deliver hydrogen far more effectively than hydrogen gas, which has very low solubility in any of the phases present.[31] The hydrogen production prevents undesirable side reactions that lead to coke and therefore leads to a lower solid residue and elevated gas production (including volatile organics).[32]

No studies have demonstrated the effective catalytic conversion of PP under HTL conditions, though for the conversion of polypropylene under higher temperatures, a number of studies have demonstrated the effective use of aluminosilicate to reduce the reaction time, lower the optimal temperature of chain scission, and support the production of a narrow range of shorter-chain hydrocarbons typical of the radical and catalytic cracking reactions.[33] In addition to the catalytic cracking of PP, aluminosilicates have also been demonstrated to be suitable for enhancing the degradation of biomass and polyolefins under pyrolytic conditions (375 °C +).[34] In this process, the cellulose derived from lignocellulosic biomass was thought to go through a sequence of dehydration, decarbonylation, and decarboxylation reactions to form furan-type compounds. These could react with olefins in the presence of zeolite through Diels−Alder reactions followed by dehydration reaction to form aromatics.[35] In addition, olefins and alkanes can act as hydrogen donors for cellulose-derived oxygenated species in the presence of a zeolite catalyst.[36] The presence of hydrogen donor solvents also aids in stabilizing the lignin radicals and stabilize reactive compounds to enhance biocrude production.[37]

However, while all of these studies were conducted under pyrolysis conditions, no studies have demonstrated the effective depolymerization of polypropylene with biomass under HTL conditions, below the supercritical point of water. Therefore, the aim of this research was to determine whether a typical thermochemical catalyst, generally used to increase biocrude yields in either HTL or pyrolysis reactions, could be further utilized to aid the breakdown of polypropylene in the co-liquefaction of biomass and PP and aid the production of further valuable products from this stream. To this end, co-processing of pistachio hull and PP was undertaken with the addition of a range of organic and inorganic catalysts and the mechanism of conversion extrapolated.

## 2. RESULTS AND DISCUSSION

**2.1. Effect of the Catalyst on the HTL Product Distribution.** While our previous work has demonstrated



https://dx.doi.org/10.1021/acsomega.0c02854
ACS Omega 2020, 5, 20586−20598

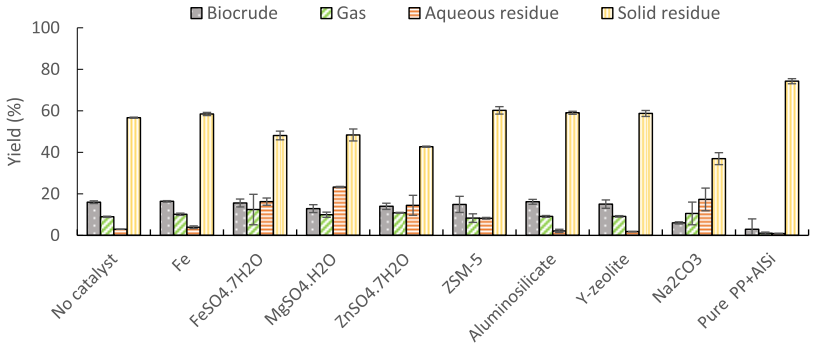


**Figure 1.** Mass balance of HTL product from the co-liquefaction of pistachio hull with 50% PP blends in the absence of catalyst and with 20% w/w of different catalysts (Fe, $FeSO_4{\cdot}7H_2O$, $MgSO_4{\cdot}H_2O$, $ZnSO_4{\cdot}7H_2O$, ZSM-5, aluminosilicate, Y-zeolite, and $Na_2CO_3$).

that HTL is a suitable process for the depolymerization of various oxygenated plastics with biomass, polyolefins are not activated by the biomass at these low temperatures, they largely do not react, and rather distribute into the solid residue intact.[17,19] In an attempt to design a system that can be used to co-process these materials, a range of commonly reported HTL catalysts were used in the co-liquefaction of 50 wt % PP blends with pistachio hulls. This loading was selected as the highest potential level of PP that would be included in a biorefinery and was demonstrated in previous studies as the optimal loading to still allow the analysis of the breakdown products even under low conversions of the initial polymer.[17−19] During hydrothermal liquefaction, the feedstock decomposed quickly to generate biocrude, aqueous residue, solid residue, and a gas phase. Mass balances are shown in Figure 1 where product yields were calculated on the basis of total feedstock input and the mass balance is the sum of the biocrude, solid, gas, and aqueous residue combined.

The biocrude production for the liquefaction of pistachio hull under these conditions was found to be 34 wt %. On the addition of 50% PP, this was reduced to 16 wt %, suggesting that the polymer is not being converted under these conditions. The biocrude yield, with additional catalysts in the co-liquefaction, resulted in a similar yield of the biocrude to the control without the additional catalyst. The yield of the biocrude product remained approximately the same (16.0 vs 16.2%) for aluminosilicate and 16.4% for Fe catalyst loading. Similarly, the yields for $FeSO_4{\cdot}7H_2O$, Y-zeolite, and ZSM-5, were 15.6, 15.1, and 14.9%, respectively. The addition of $Na_2CO_3$ was found to deplete the biocrude substantially, with yields decreasing from 16.0 to 6.0%.

Similarly, the gas phase product obtained from the presence of the catalysts was comparable to those obtained for 50 wt % PP blends with pistachio hulls without the catalyst. The yield of the gas phase products increased from 8.9% for the noncatalytic reaction to 12.4, 10.9, 10.2, and 10.0% for $FeSO_4{\cdot}7H_2O$, $ZnSO_4{\cdot}7H_2O$, Fe, and $MgSO_4{\cdot}H_2O$, respectively, but a small reduction was observed for the aluminosilicate and zeolite-type catalysts. This strongly suggests that the PP is not being cracked into volatile organics species under these conditions.

For the aqueous phase residue yield, a modest increase was found with the addition of $MgSO_4{\cdot}H_2O$ (23.5%) as well as with $Na_2CO_3$ (17.3%), $FeSO_4{\cdot}7H_2O$ (16.2%), $ZnSO_4{\cdot}7H_2O$ (14.5%), and ZSM-5 (14.5%) from 2.9% for the noncatalyzed reaction. In contrast, the aqueous phase residue yield was not significantly impacted by the addition of aluminosilicate, Y-zeolite, and Fe.

The co-liquefaction of PP with pistachio hull mainly contributed to an increase in the solid residue with both the presence and absence of the catalyst. The most significant impact was observed for co-liquefaction of 50% PP blends with pistachio hull and ZSM-5, with an increase in the solid residue yield from 56.7 to 60.2%. The high solid recovery was observed following the addition of aluminosilicate, Y-zeolite, and Fe (solid residue yields of 59.1, 58.7, 58.5%, respectively), which were similar to those obtained for 50% PP blends in pistachio hull without catalyst loading. In contrast, the solid residue phase yield decreased with the addition of $MgSO_4{\cdot}H_2O$, $FeSO_4{\cdot}7H_2O$, $ZnSO_4{\cdot}7H_2O$, from 56.7 to 48.3, 48.1, 42.7%, respectively, and substantially decreased to 37% for $Na_2CO_3$ loading.

Irrespective of the catalyst, the polypropylene did not break down and distribute into the crude phase and rather distributed into the solid residue phase. The reason is either the polymer is not reacting, as previous studies have demonstrated,[19] or that it is breaking down into a solid such as elemental carbon. To check the synergistic effect of co-liquefaction of biomass and plastic with and without the catalyst, pure PP was also reacted under these conditions. The synergistic effect of the interaction between biomass and plastics can be determined through the equation

$$\text{synergistic effect} = Y_{BC} - (X_{PWPP} \times Y_{PWPP} + (1 - X_{PP}) \times Y_{PP})$$

where $Y_{BC}$ is the yield of the biocrude obtained in the experiment, $X_{PWPP}$ is the mass fraction of pistachio hull and PP in the total reaction mixture, $X_{PP}$ is the mass fraction of pure PP, $Y_{PWPP}$ is the biocrude yield of pistachio hull with 50% blend PP without the catalyst, and $Y_{PP}$ is the biocrude yield of pure PP.

Some synergistic effect for the co-liquefaction of biomass with PP was observed for all of the catalysts except $Na_2CO_3$ (Figure 2a). The positive correlation was observed for the total biocrude yield, with the highest positive correlation of 3.6% for the presence of Fe. A lower synergistic effect was observed with aluminosilicate (3.4%). The presence of $FeSO_4{\cdot}7H_2O$, $ZnSO_4{\cdot}7H_2O$, ZSM-5, and Y-zeolite all had a lower effect on the conversion of 2.8, 1.2, 2.1, and 2.3%, respectively. The smallest positive correction was found for the presence of $MgSO_4{\cdot}H_2O$ (0.1%).

**2.2. Product Characterization.** *2.2.1. Biocrude Composition.* The initial mass balance suggests that if the polypropylene is breaking down, then it is not distributing substantially into the biocrude. Further analysis of the biocrude


https://dx.doi.org/10.1021/acsomega.0c02854
ACS Omega 2020, 5, 20586−20598

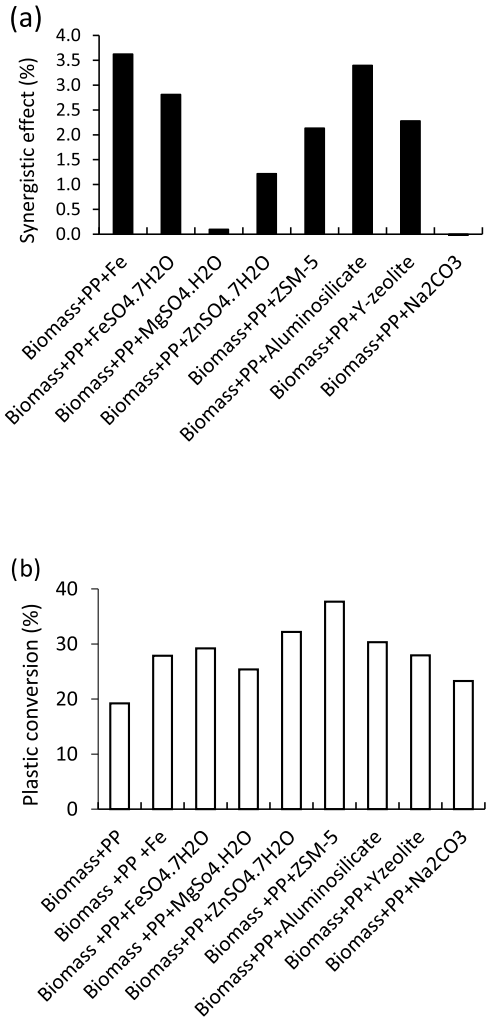


**Figure 2.** (a) Synergistic effect of the biocrude obtained from pure PP with aluminosilicate and co-liquefaction of PP/biomass with different catalysts. (b) Extent of plastic conversion at 350 °C, calculated using Fourier transform infrared (FT-IR) (see the Supporting Information for further details).

supports this conclusion, with the elemental composition not changing substantially relative to biocrude produced without a catalyst (Figure 3a). All of the biocrudes were characterized by high carbon content, similar hydrogen levels, and reasonably low alternative elements; this suggests that the biocrude was largely unchanged by the addition of the catalysts in this system and that the catalysts all distributed largely into other phases. As such, the energy content distributing into the crude remains relatively low.

To examine the effect of the additional catalyst on the biocrude composition, the biocrudes produced from the co-liquefaction of pure pistachio hull, biomass/PP blends, and 20 wt % aluminosilicate in biomass/PP blends were characterized by gas chromatography−mass spectrometry (GC−MS). The major compounds (quality >80%) of the biocrude oils are summarized in the Supporting Information (Table S5). From the GC−MS analyses, more than 50 compounds were observed in each biocrude sample. The chemical composition of the biocrude product fraction is connected mainly with the origin of the biomass. Some alkanes were observed in high amounts in the presence of PP blends and seem to be formed by specific interactions with the addition of the catalyst. Each biocrude contained several phenolic compounds, these presumably originate from lignin, which is one of the major components of the pistachio hulls. Additionally, the major chemical compositions were detected in the level of carboxylic acid compounds such as 3-cyclohexene-1-carboxylic acid and alkane compounds such as decane 4-ethyl, decane 2,4-dimethyl. Similar changes were found in previous work by the co-pyrolysis of biomass with PP,[38] which suggests that there is some, albeit very limited, breakdown of the PP into hydrocarbons.

For the presence of PP, a small increase in ketone and ester formation was also observed. Additionally, increased levels of ethanone, benzo-furan, carboxylic acids, ester, and methyl ester were present. These compounds were not found from the biocrude derived from pure pistachio hull, suggesting that the co-liquefaction with PP blends can affect the chemical composition of biocrude oil. In a previous study, Coma et al. demonstrated that ketones and esters were formed in the breakdown of polyethylene with microalgae,[18] suggesting that these are formed by the limited breakdown of PP catalytically.

For the presence of the catalyst (aluminosilicate), an increase in carboxylic acids and fatty acids was observed. These results indicate the interaction and synergistic effect of aluminosilicate catalytic HTL during co-processing of biomass with the PP blends. However, 2,4-dimethylhept-1-ene, a typical breakdown species for polypropylene formed during pyrolysis,[39,40] was not observed, suggesting that the mutual influence of co-liquefaction of biomass and PP during the thermal decomposition was not completed. These findings were also confirmed in the study of the functional groups in the solid residue through FT-IR with the presence of unreacted PP.

The biocrude $^1$H NMR spectra are given in the supporting information (Figure S3). While exceptionally complex, specific regions, relating to the functional groups, were integrated and divided into 5 ppm ranges (Figure 4). The $^1$H NMR results showed that the resulting biocrude was of a similar bulk composition when obtained from co-liquefaction in both the presence of the catalyst and without the catalyst. $^1$H NMR showed a high percentage of the alkane functional groups for biocrude oil; this suggests that the contribution of the alkane compounds was derived from the decomposition of triglycerides of pistachio hull during HTL processing. The addition of Y-zeolite demonstrated the highest alkanes (48.2%) and alcohol functionality (30%) but the lowest percentage of $\alpha$-to-heteroatom functionality (22%), this suggests that there a is low nitrogen content in these samples. The presence of aluminosilicate had the highest percentage of $\alpha$-to-heteroatom functionality (23.6%), which was approximately the same as with ZSM-5 (23.2%). All biocrudes presented a low percentage of the aromatic and the methoxy functionality (0.0−0.2%), which are consistent with carbohydrates converting into biocrude, and the catalyst not cracking polypropylene and reforming as aromatic species.

*2.2.2. Aqueous Residue Characterization.* The co-liquefaction with additional catalysts reduced the carbon and nitrogen content in the resulting aqueous phase (Table 1). The total organic carbon and total nitrogen in the aqueous product phase are distributed very similarly, with the range of 5.2−9.7 g $L^{-1}$ for carbon concentration and 0.3−0.7 g $L^{-1}$ for nitrogen. This suggests that the breakdown of PP is not producing water-soluble species that are distributing into the aqueous phase.


https://dx.doi.org/10.1021/acsomega.0c02854
ACS Omega 2020, 5, 20586−20598

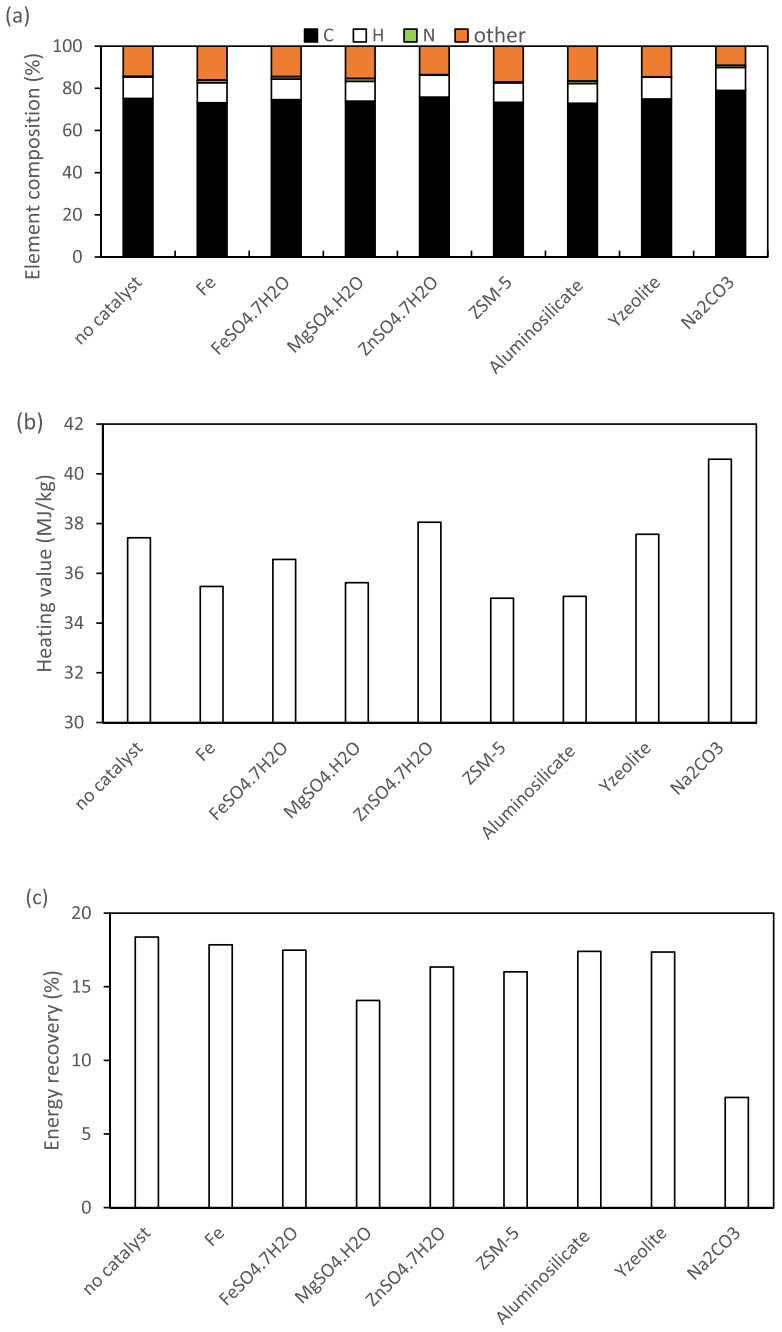


**Figure 3.** (a) Elemental composition (determined by elemental analysis), (b) heating value of the biocrude, and (c) energy recovery of the biocrude of 20 wt % catalyst loading.

The only significant difference is the aqueous phase produced by the co-liquefaction with $Na_2CO_3$, which shows a substantially increased carbon content, and slightly increased nitrogen content in the aqueous phase at 30.0 and 1.0 g $L^{-1}$, respectively. This is presumably due to the formation of carbonic acid and sodium hydroxide with the decomposition of $Na_2CO_3$ in water.

*2.2.3. Solid Residue Composition.* The FT-IR spectra of the solid residue demonstrate that a large proportion of the PP is breaking down; however, hardly any typical breakdown products are observed in the biocrude or the aqueous phase, the gas phase also remains constant. It is therefore likely that the breakdown products are distributing into the solid residue itself.

All FT-IR spectra of the solid residue produced are present in the Supporting Information (Figure S1a–h). Generally, the spectra all show a similar intensity of peaks corresponding to the stable compounds formed during the HTL process. Those produced show an intensive absorbance at ∼2800–3000 and ∼1300–1500 $cm^{-1}$, suggestive of an aliphatic functional group and aromatic group, respectively. However, the intensity of these peaks decreased slightly in the solid residue produced from the addition of Fe, ZSM-5, aluminosilicate, and Y-zeolite. These results suggest that there is a synergistic interaction between those catalysts, thus improving decomposition.


https://dx.doi.org/10.1021/acsomega.0c02854
ACS Omega 2020, 5, 20586–20598

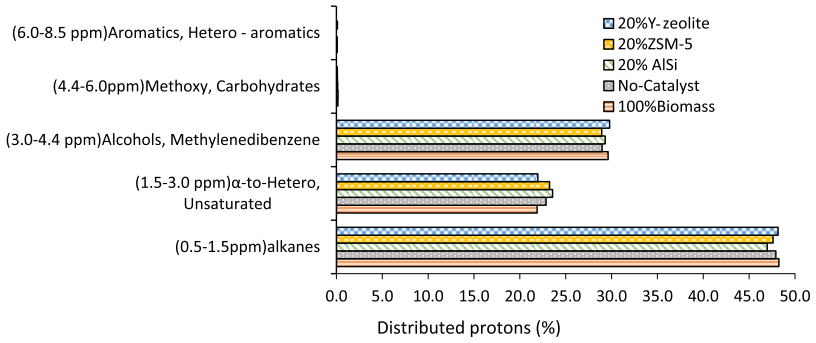


**Figure 4.** $^1$H NMR spectroscopy results of the percentage of the integrated peak area regions for each range of parts per million (ppm) with respect to the total integral.

**Table 1. Elemental Composition of the Aqueous Phase Produced from Co-liquefaction of Polypropylene**

| sample | TOC (g $L^{-1}$) | TN (g $L^{-1}$) |
|---|---|---|
| 50% PP and biomass | 9.7 | 0.7 |
| 20% aluminosilicate | 7.0 | 0.5 |
| 20% ZSM-5 | 6.3 | 0.3 |
| 20% Y-zeolite | 6.2 | 0.5 |
| 20% $Na_2CO_3$ | 30.4 | 1.0 |
| 20% Fe | 6.5 | 0.6 |
| 20% $FeSO_4{\cdot}7H_2O$ | 5.2 | 0.5 |
| 20% $ZnSO_4{\cdot}7H_2O$ | 6.7 | 0.6 |
| 20% $MgSO_4{\cdot}H_2O$ | 7.1 | 0.5 |

However, the addition of those catalysts did not significantly breakdown polymer blends/biomass into the biocrude, they were mostly broken down into the solid residue with the most likely compounds being aromatic species and elemental carbon.

Overall, the elemental composition changed during thermal HTL processing. All solid residue products had a higher C content and a lower O/H ratio than the raw material used (Figure 5a), which suggests that dehydration and polymerization occurred during the HTL process. Compared to the co-liquefaction of biomass with PP without a catalyst, the C content slightly decreased from 84.7 to 83.8, 78.9, 78.8, and 78.6% for $Na_2CO_3$, $FeSO_4{\cdot}7H_2O$, $ZnSO_4{\cdot}7H_2O$, and $MgSO_4{\cdot}H_2O$, respectively. In contrast, the C content decreased substantially from 84.7 to 66.6, 63.1, 62.0 and 54.3% for aluminosilicate, Fe, ZSM-5, and Y-zeolite, respectively. This result can be confirmed by the appearance of the peaks at ~2920 and 2850 $cm^{-1}$ and ~1400 $cm^{-1}$ during liquefaction as proposed in the FT-IR spectra. These intensive peaks enhanced the C content of the solid residue, which strongly suggests the presence of the unreacted polymer. The N content was not significantly impacted by any of the additional catalyst loadings, with a similar N content of 0.1−0.5% for each experiment. The addition of Y-zeolite caused the H content to decrease substantially from 14.3 to 8.5%, while the addition of aluminosilicate, ZSM-5, and Fe caused the H content to decrease from 14.3 to 11.0, 10.5, and 10.0%, respectively. The O content again was not strongly affected, with a slight increase of 2.2−4.0% with the exception of $Na_2CO_3$ (a decrease from 2.2 to 1.2%).

The higher heating values (HHVs) of the solid residue produced were calculated (Figure 5b). Presumably due to the low oxygen content, the solid residue produced from co-liquefaction of 50% PP blends/biomass without the catalyst showed the highest HHVs observed at 48.7 MJ $kg^{-1}$. Reduced HHVs were observed at 48.1, 43.7, 43.5, 43.2 MJ $kg^{-1}$ for $Na_2CO_3$, $FeSO_4{\cdot}7H_2O$, $MgSO_4{\cdot}H_2O$, and $ZnSO_4{\cdot}7H_2O$, respectively. A substantial reduction in the HHV was observed for the other solid residues produced with Fe (34.4 MJ $kg^{-1}$), aluminosilicate (37.1 MJ $kg^{-1}$), ZSM-5 (35.3 MJ $kg^{-1}$), and Y-zeolite (29.8 MJ $kg^{-1}$). This is highly suggestive that the polypropylene is breaking down somewhat into a less energy-dense material with the alternative catalysts as opposed to the noncatalytic residue, which has an HHV very similar to PP. Because of its high heating value, the solid residue obtained from the co-liquefaction of pistachio hull and PP in the addition of the catalyst could potentially be used as a solid fuel.

Van Krevelen diagrams of the solid residues are used to determine the degree of aromaticity and maturation during thermochemical degradation. During the HTL process, some of the oxygen in the biomass is removed in the form of $H_2O$ (dehydration) or $CO_2$ (decarboxylation). A reduction of H and O content in the substance can be defined by the H/C and O/C ratios. The diagram shows the comparison of biomass with peat and lignite, brown coal, coal, and anthracite. The H/C ratio is related to the degree of carbonization, where the O/C is also a useful measure of the surface hydrophilicity due to O relating to polar-group content.[41−43] While the amount of PP in the samples obviously makes these solids difficult to compare with the alternative biomass samples in the literature, the comparison across the data set is illuminating. Overall, H and O were exhausted in the bioresidues examined and it became carbon-rich during hydrothermal liquefaction. The O/C ratios of the solid residue produced were substantially increased compared to the raw feedstock (Figure 6). The O/C ratio of the solid residue produced was very low, presumably in part due to the unreacted PP in the solid, with O/C ratios of 0.01−0.1 observed. The lower O/C ratio showed more aromatic and less hydrophilic content of the solid residue produced due to a higher degree of carbonization and extinction of polar functional groups during hydrothermal processing. For the H/C ratio, the co-liquefaction of 50% blend PP/biomass without the catalyst and the addition of the catalysts provided a similar level of the H/C ratio (0.16−0.17).

So, while, the solid residue could be combusted akin to a coal product, the presence of PP in the sample would still be problematic from a regulatory point of view.[44] However, potentially a higher value route might be to use the solid remediator as a soil remediation fertilizer. The high carbon content of the solid residue can provide beneficial properties for maximizing the amount of carbon storage[45] and in effect takes fossil carbon from the PP and converts it into a


https://dx.doi.org/10.1021/acsomega.0c02854
ACS Omega 2020, 5, 20586−20598

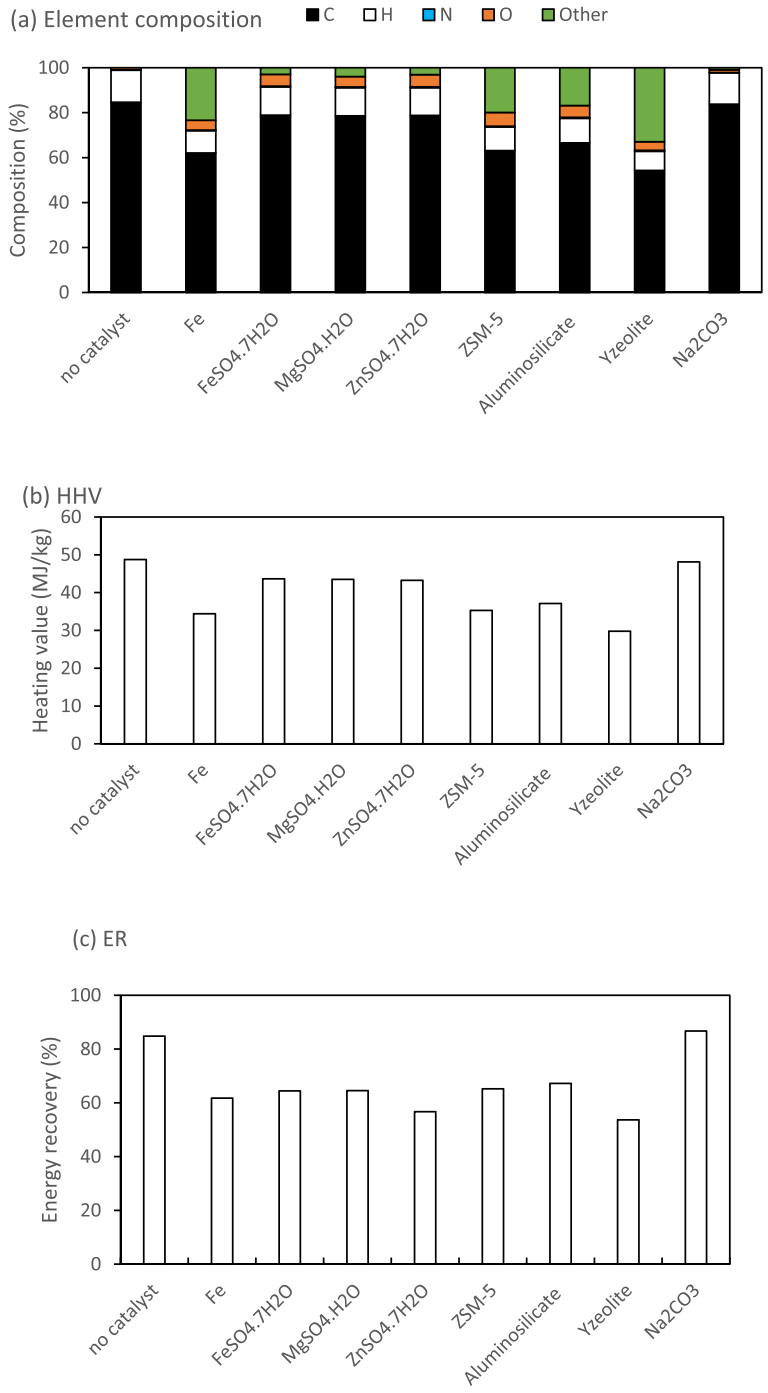


**Figure 5.** (a) Elemental composition of the solid residue of 20 wt % different catalyst loading, (b) heating value, and (c) energy recovery (%).

bioavailable, long-term carbon storage option when coupled with reforestation.[46]

**2.3. Enhancing the Liquefaction of PP and Biomass.** Due to the lower HHV of the solid residue, higher conversion rates, and low cost, aluminosilicate was taken forward as a suitable catalyst for further development. High crude yields from biomass are generally achieved with a very fast heating rate and short reaction time;[47] however, the exact mechanisms of the HTL still remain unclear mainly due to the complexity of the feedstock and HTL products.[48] While high heating rates favor higher crude production, a slower heating rate may possibly affect the decomposition of plastic and increase overall biocrude yields.[49] The experiments were therefore conducted using slower heating rates of 7.7 °C $min^{-1}$ with the total time of 45 min for the co-liquefaction of PP/biomass with the presence of aluminosilicate. As the reaction time increased, the biocrude oil yield did not increase significantly (Figure 7a), solid residue and gaseous products from all long reaction times also produced similar results. This finding indicates that a long reaction time was not an essential factor in the depolymerization of PP in this study.

HTL was also carried out at this lower heating rate and rapid heating rates (33 °C $min^{-1}$) over different temperatures (250, 300, and 350 °C) and gave rise to lower overall conversions of


https://dx.doi.org/10.1021/acsomega.0c02854
ACS Omega 2020, 5, 20586−20598

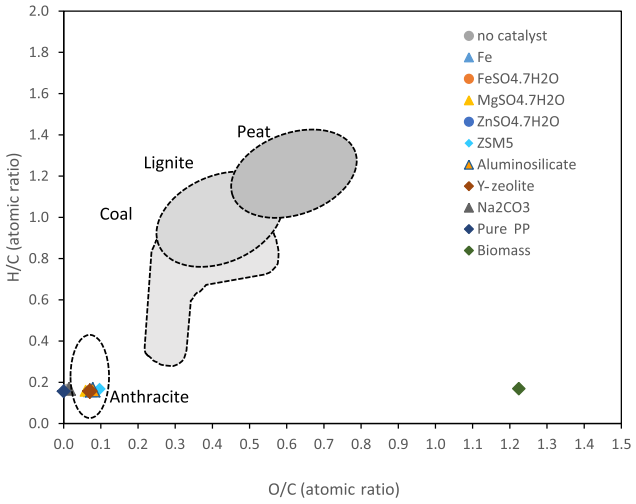


**Figure 6.** Van Krevelen diagram with the H/C and O/C molar ratios of various catalysts and without catalysts for co-liquefaction of polypropylene and pistachio hull.

plastics in all cases with the exception of reaction temperature at 350 °C (increase from 17 to 26% conversion for slow heating rates). This indicates that faster heating rates are preferred for balancing both overall biocrude yield and plastic conversion. This demonstrates the synergistic effect of processing the PP with biomass and using a catalyst, as there is no appreciable conversion of PP at this temperature range when PP is added to water alone.

Despite the catalysts improving the conversion yield substantially compared to the noncatalytic route, the mechanism of conversion remains unclear. To assess the major pathway for the liquefaction, three further organic additives were used in the aluminosilicate-catalyzed reaction of PP and pistachio hull. First, the co-liquefaction of biomass/PP blends with the aluminosilicate catalyst was undertaken in the presence of formic acid. Formic acid has been demonstrated to give higher crude yields in the HTL of microalgae[30] and breaks down into $H_2$ and $CO_2$ under high temperatures as well as acting as an acid catalyst, which increases the interaction of soluble HTL products during hydrothermal liquefaction and prevents undesirable side reactions, which has been shown to lead to lower solid residues and an increase in gas production.[32] As such, in the liquefaction of lignin, formic acid has been demonstrated to increase bio-oil yields, decreasing the amount of carbon that goes into the solid residue.[31]

Another possible mechanism is the free-radical decomposition; to investigate this, a stable radical donor (hydrogen peroxide, $H_2O_2$) was added, and this was compared to the radical scavenger antioxidant: butylated hydroxytoluene (BHT). Hydrogen peroxide has been applied for enhancement of liquid yield from liquefaction to many types of biomass, aiding in the generation of radicals.[50−52] During liquefaction, the hydrogen peroxide can oxidize unsaturated side chains and crack aromatic rings, leading to an improvement of the depolymerization and enhancement of the degradation in the solvent effectively.[51,53,54] Besides, hydrogen peroxide gives a source of radicals that may aid the radical scission of the PP chain.

The product distribution and PP conversion are given in Figure 8a. The addition of FA showed the biocrude obtained increased from 12.0 to 20.0%, while slightly increased from 12.0 to 14.1% with the presence of hydrogen peroxide, but the biocrudes remained unchanged in the presence of BHT. The gas yield was significantly impacted by the addition of formic

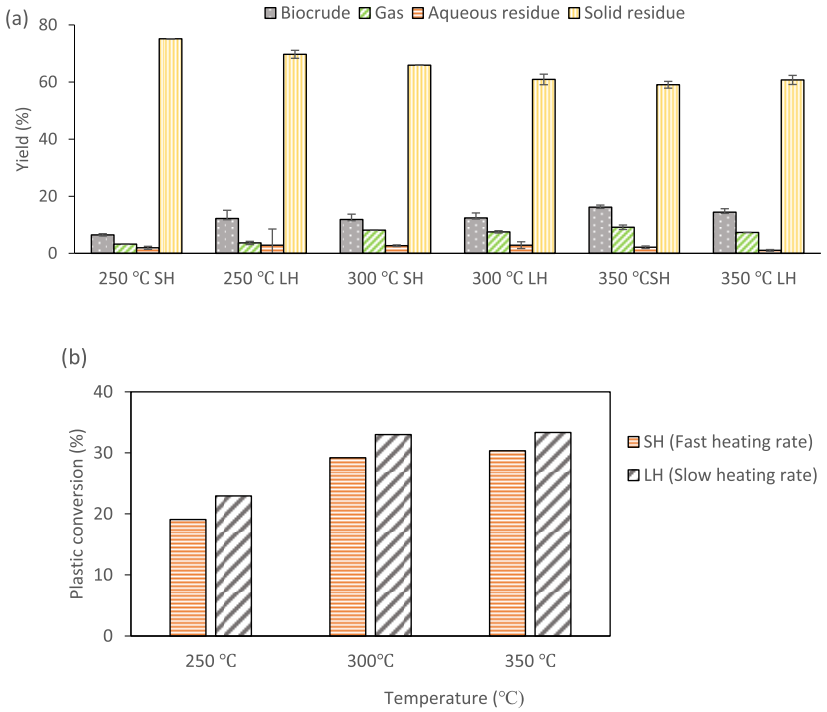


**Figure 7.** (a) Effect of the faster heating rate on product yield and mass balance on different temperatures and reaction rates of faster heating rate (SH) and slow heating rate (LH) for the aluminosilicate-catalyzed HTL conversion of PP and pistachio hulls; (b) the estimated plastic conversion for the same system calculated through FT-IR.



https://dx.doi.org/10.1021/acsomega.0c02854
*ACS Omega* 2020, 5, 20586−20598

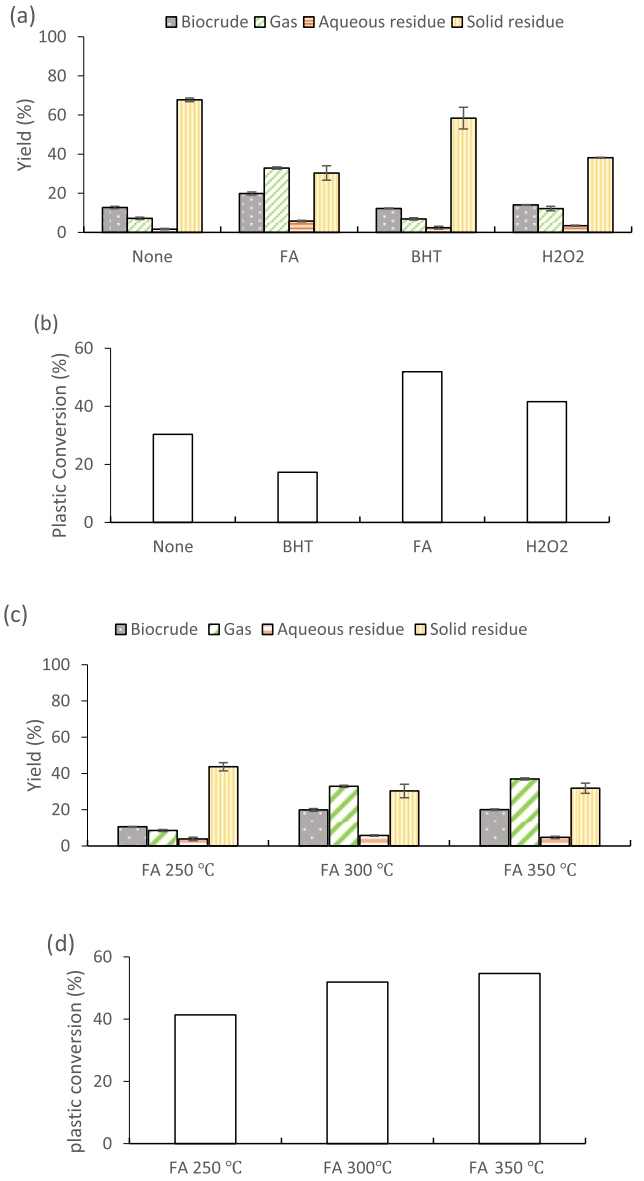


**Figure 8.** (a) Effect of the addition of FA, $H_2O_2$, and BHT on the product yield distribution on co-liquefaction biomass with 50 wt % PP blends with 20% aluminosilicate loading at 300 °C and 10 min reaction time, (b) plastic conversion (%). (c) Effect of the addition of formic acid (FA) on the product yield distribution with different temperature and (d) plastic conversion (%) of the addition of FA.

acid and increased from 7.2 to 33.0%. Gas yields also increased in the presence of $H_2O_2$, from 7.2 to 12.2%, but remained unchanged in the presence of BHT. These findings suggest that formic acid is breaking down into $CO_2$ and $H_2$, which has led to the increase in gas fraction, as previously observed.[20] However, this would give a theoretical increase of gas phase product yields to approximately 29.4%, assuming no hydrogen reacts with the products, much lower than observed, suggesting an increased breakdown of biomass and PP into the gas phase. This was confirmed with a range of over 150 volatile organic compounds (VOCs) observed by gas phase GC−MS (see the Supporting Information); this effect was also observed in the liquefaction of lignin with formic acid in ethanol.[55]

The amount of the solid residue substantially decreased from 67.8% for the catalyzed process to 30.3% with the addition of formic acid and to 38.2% with the addition of $H_2O_2$. The presence of FA and $H_2O_2$ in the HTL reactions decreased the solid residue formation substantially, suggesting that both the addition of hydrogen and the generation of free radicals aided the decomposition of the PP chain, through either a cracking or free-radical scission reaction, that produced elevated levels of VOC in the gas stream. The role of the free-radical mechanism was further demonstrated by reducing the polymer scission on the addition of BHT.

To optimize the system further, formic acid was added to the aluminosilicate-catalyzed reaction at 250, 300, and 350 °C (Figure 8c). At a reaction temperature of 250 °C, the biocrude yields tended to decrease concomitantly with solid residue formation decreasing. A substantial increase in the biocrude yield was observed when the reaction was performed at 300 °C, with the solid residue product reduced. However, the reaction at 350 °C did not result in higher biocrude yields obtained compared to 300 °C but a slight increase was found in terms of gas phase formation.

On analysis, the condensable gas phase was found to contain over 164 C3−C10 compounds. Over 60% of these were hydrocarbons, with 33% of the total compounds being branched or linear alkanes and alkenes, this contained significant proportions of branched C7−C10 fragments, including high levels of 2,4-dimethylhept-1-ene, other substituted C9 alkenes, and propylene (full analysis is given in the Table S6 and Figure S4 in the Supporting Information). The amount of unsaturated species in the volatile phase supports a free radical or catalytic cracking mechanism.

The presence of aluminosilicate facilitates the cracking of polypropylene due to the high surface area and acidity, with the pore size providing some shape selectivity for small species. The addition of the hydrogen donor further enhances the cracking and hydrogenation reactions. Therefore, the incorporation of the formic acid seems to aid the fluid catalytic cracking reaction, leading to a range of low MW alkenes as the final product. Since polypropylene degradation takes place initially on the external surface of the catalyst and disperses into small internal cavities of the catalyst, they further degraded to the small size of gaseous hydrocarbons, particularly isoalkanes and alkenes. This is supported by the product profile, which is consistent with other similar pyrolysis studies, where a high content of volatile hydrocarbons was achieved from cracking over the acidic aluminosilicate catalyst.[28,33] These results suggest that PP can be thermally depolymerized under these conditions forming a range of alkene fragments suitable for further valorization either to recombine into an upcycled polyolefin polymer or combine with the crude for further hydroprocessing into a fuel.

## 3. CONCLUSIONS

Increasing plastic contamination in biomass waste streams is a significant issue, which interferes with the traditional fuel processing routes. Here, we report a possible solution through the catalytic co-liquefaction of biomass and polypropylene. Previous work demonstrated that in water alone below 370 °C, there is no appreciable conversion of PP, with the addition of biomass, a synergistic effect does occur but leads to very low conversions (<10%). In this study, the effect of using an additional catalyst in the hydrothermal liquefaction of biomass with polypropylene was investigated for the first time. The biocrude was largely unchanged by the addition of the catalysts in terms of the elemental composition; however, using aluminosilicate species, a large proportion of the polymer


https://dx.doi.org/10.1021/acsomega.0c02854
ACS Omega 2020, 5, 20586−20598

could be converted into a solid residue suitable for use as a possible solid fertilizer or further energy product. The activity could be further enhanced by adding either a radical promotor or the organic hydrogen donor formic acid. This reduced the amount of fossil carbon going to the solid fraction and rather volatile organic species were predominantly produced, with the majority of the components being C3−C10 branched hydrocarbon fragments. The ability to stop the reaction through the addition of BHT demonstrated the importance of a radical mechanism for the depolymerization. This work demonstrates that it is possible to combine polyolefins in an HTL biorefinery, though catalysis and additional radical producers are needed to produce a suitable range of products. This volatile organic carbon stream could be used to produce further polyolefins in a circular economy methodology or be combined with the crude product and hydrotreated to add to the total liquid energy product produced from this system. Future studies should therefore aim to assess the viability of adding hydrogen and radical donors to the HTL system.

## 4. MATERIAL AND METHODS

**4.1. Feedstock Sources and Characterization.** Pistachio hull was selected as a representative of agriculture waste based on our previous work in this area and the relatively high lipid and protein content of the feedstock.[19] Pistachio hull biomass (3 mm particle size) was sourced as a waste material after pistachio processing from the Wonderful Company, CA. The full characterization is given in the Supporting Information. Polypropylene (PP) was selected as the fossil-based plastic, with an average molecular weight number $M_W$ = 12 000 g mol$^{-1}$, was sourced from Sigma-Aldrich, and ground to a particle size of <350 $\mu$m. Iron (Fe), $FeSO_4{\cdot}7H_2O$, $MgSO_4{\cdot}H_2O$, $ZnSO_4{\cdot}7H_2O$, aluminosilicate, Y-zeolite, $Na_2CO_3$, hydrogen peroxide, and butylated hydroxytoluene were all purchased from Sigma-Aldrich and used without further purification. ZSM-5 (Zeolyst CBV 3024E) was purchased from Zeolyst International and used without further treatment or purification. Formic acid was purchased from Fisher Chemicals and used without further purification. Further material analysis is given in the Supporting Information (Table S1).

**4.2. Co-processing Hydrothermal Liquefaction.** Co-hydrothermal liquefaction of multiple solid wastes was carried out using a stainless-steel batch reactor of 50 mL. According to a previous relevant study,[17] the reactor was equipped with a pressure gauge and pressure relief valve and a needle valve to release the gaseous products. The temperature was monitored using a thermocouple inside the reactor, placed half-way down the length, was connected to data logging software, and used to control the temperature of the reaction. The experiments contained either 1.5 g of PP and 1.5 g of pistachio hull for the control experiments or 1.2 g of PP, 1.2 g of pistachio hull, and 0.6 g of the catalyst (either Fe, $FeSO_4{\cdot}7H_2O$, $MgSO_4{\cdot}7H_2O$, $ZnSO_4{\cdot}7H_2O$, ZSM-5, aluminosilicate, Y-zeolite, or $Na_2CO_3$). This gave a total catalyst loading of 20% w/w of the overall mixture in the reactor. For the further additive experiments, 0.65 g of formic acid (FA), 0.5 g of hydrogen peroxide ($H_2O_2$), or 0.02 g of butylated hydroxytoluene (BHT) were mixed with 15 g of distilled water to form a slurry feedstock; this was then added to the 3 g of total solids. A total of 18 g of slurry feedstock was therefore loaded into the reactor for each reaction and the reactor was sealed and loaded into a preheated furnace to 800 °C (rapid heating rate) or 600 °C (lower heating rate).

As reaction time is also considered to play an important role in the product fraction and HTL pathway; the reactor was held in the furnace until the temperature reached 350 °C for either 10 min (furnace temperature of 800 °C, heating rate of 33 °C min$^{-1}$) and 45 min (furnace temperature of 600 °C, heating rate of 7.7 °C min$^{-1}$). Upon reaching the desired temperature, the reactor was removed from the furnace rapidly and allowed to cool to room temperature. Each experiment was repeated at least three times to determine the average values and the standard deviation. Both the reactor setup and examples of the temperature profile for the reactions are given in the Supporting Information. The pressure is generated predominantly by the water being heated and reached approximately 165 bar under the conditions tested at 350 °C, 100 bar at 300 °C, and below 45 bar at 250 °C.

**4.3. Separation of the Liquefied Product.** After cooling, the gaseous products were released via the needle valve into an inverted, water-filled measuring cylinder to determine the total gas volume. The gas phase yield was determined according to the literature precedent, by using the ideal gas law and assuming that the gas was completely $CO_2$.[25] The liquid−solid mixtures were filtered through a filter paper to separate the aqueous phase from the water-insoluble fraction (consisting of the biocrude and solid residue). The solid−liquid mixture remaining on the filter paper was washed repeatedly with chloroform until the solvent was clear. The chloroform was removed using a rotary evaporator at 40 °C for 1.5 h to isolate the biocrude. The solids were oven-dried overnight at 60 °C to determine the solid-phase product yield as the "solid residue". An aliquot of the aqueous phase products was dried overnight at 60 °C to determine the yield of nonvolatile organics and inorganics in the aqueous phase, designated as the "aqueous residue".

**4.4. HTL Product Characterization.** *4.4.1. FT-IR and $^1$H NMR.* Functional group information in the solid-phase and biocrude products was derived through FT-IR and NMR spectroscopic data. The FT-IR spectra were recorded using a Thermo Scientific Nicolet iS5 FT-IR spectrometer in the wavenumber range from 4000 to 600 cm$^{-1}$. FT-IR was also used to assess the level of unreacted plastic remaining in the solid-phase products as a proxy for the extent of plastic conversion (the same method reported in our previous works[19]).

$^1$H NMR spectra were collected using a Bruker Avance III NMR spectrometer operating at 500.13 MHz, using TopSpin 3.5. The samples were prepared by dissolving biocrude oil in deuterated chloroform. The samples were then filtered to remove any suspended particulates before loading into the NMR tubes. The spectra were obtained using the zg30 pulse sequence, with td = 65 536 and ns = 16 and a relaxation delay of 1 s.

*4.4.2. Elemental Composition and Energy Recovery.* Elemental analysis of the biomass feedstock and products was conducted at London Metropolitan University. The samples were processed for carbon, hydrogen, and nitrogen on a Carlo Erba Flash 2000 elemental analyser. Oxygen analysis of the solid residue was analyzed at Elemental Microanalysis in Devon, U.K. The higher heating values (HHVs; MJ kg$^{-1}$) of the biomass, solid residue, and biocrude were calculated using the Dulong formula[29,56,57] based on the elemental composition; HHV = 0.3383C + 1.422 × (H−O/8). The energy recovery in each product phase was calculated as the biocrude divided by that combined feedstock; energy


https://dx.doi.org/10.1021/acsomega.0c02854
ACS Omega 2020, 5, 20586−20598

recovery = HHV product (%) × mass of product (%)/HHV of feedstock (%).

*4.4.3. Biocrude Composition by Gas Chromatography–Mass Spectroscopy (GC–MS).* The chemical composition of the volatile fraction of the biocrude was identified by comparing the mass spectra with those in the NIST mass spectral database using an Agilent Technologies 8890 GC system fitted with a 30 m × 250 μm × 0.25 μm HP5-MS column, coupled to a 5977B inert MSD. The samples were dissolved in tetrahydrofuran (THF), and helium (1.2 mL $min^{-1}$) was used as the carrier gas. The initial oven temperature was set to 50 °C, increasing to 250 °C at 10 °C $min^{-1}$.

*4.4.4. Gas Analysis by Gas Chromatography–Mass Spectroscopy (GC–MS).* Approximately 50 mL of each gas sample was collected to a Tenax tube (TA 200 mg 35/60 mesh inert coated conditioned stainless-steel TD tube) and analyzed using a TD100-XR GC system coupled to an 8890 gas chromatograph (Agilent) with 5977B MSD (Agilent). The column was Agilent HP-5MS (30 m, 0.25 mm, 0.25 μm). Pretrap fire purging was performed for 1 min, after which the trap was fired at 300 °C for 3 min. Split flow during trap desorption was 50 mL $min^{-1}$, resulting in a split ratio of 42:1. Helium was applied as a carrier gas at 1.2 mL $min^{-1}$. The column program was started at 40 °C, which was held for 7 min, and increased at a rate of 10 °C $min^{-1}$ to 150 °C and then 40 °C $min^{-1}$ to 325 °C, which was held for 7 min, giving a total run time of 27.3 min.

## ■ ASSOCIATED CONTENT

### Supporting Information

The Supporting Information is available free of charge at https://pubs.acs.org/doi/10.1021/acsomega.0c02854.

Further biomass composition, FT-IR spectra of the solid residue, calibration curves for estimating plastic conversion, GC–MS analysis of the biocrude, NMR analysis of the biocrude, gas analysis, reactor schematic and heating profile (PDF)

## ■ AUTHOR INFORMATION


### Corresponding Author

**Christopher J. Chuck** − *Department of Chemical Engineering, University of Bath, Bath BA2 7AY, U.K.;* orcid.org/0000-0003-0804-6751; Email: c.chuck@bath.ac.uk

### Authors

**Sukanya Hongthong** − *Department of Chemical Engineering, University of Bath, Bath BA2 7AY, U.K.*

**Hannah S. Leese** − *Department of Chemical Engineering, University of Bath, Bath BA2 7AY, U.K.*

Complete contact information is available at: https://pubs.acs.org/10.1021/acsomega.0c02854


### Author Contributions

S.H. completed the experimental data collection, H.S.L. and C.J.C. conceived the study and supervised the work undertaken. The manuscript was written through the contributions of all authors. All authors have given approval to the final version of the manuscript.

### Notes

The authors declare no competing financial interest.

## ■ ACKNOWLEDGMENTS

The authors would like to acknowledge the Royal Thai Scholarship for funding the Ph.D. studentship (Sukanya Hongthong) and Dr. Tim Woodman for his help with the NMR analysis through the Materials and Chemical Characterisation facility at the University of Bath ($MC^2$).

## ■ REFERENCES


(1) Thompson, R. C.; Moore, C. J.; vom Saal, F. S.; Swan, S. H. Plastics, the environment and human health: Current consensus and future trends. *Philos. Trans. R. Soc., B* **2009**, *364*, 2153−2166.

(2) Marin, N.; Collura, S.; Sharypov, V. I.; Beregovtsova, N. G.; Baryshnikov, S. V.; Kutnetzov, B. N.; Cebolla, V.; Weber, J. V. Copyrolysis of wood biomass and synthetic polymers mixtures. Part II: characterisation of the liquid phases. *J. Anal. Appl. Pyrolysis* **2002**, *65*, 41−55.

(3) Block, C.; Ephraim, A.; Weiss-Hortala, E.; Minh, D. P.; Nzihou, A.; Vandecasteele, C. Co-pyrogasification of Plastics and Biomass, a Review. *Waste Biomass Valorization* **2019**, *10*, 483−509.

(4) Sharypov, V. I.; Marin, N.; Beregovtsova, N. G.; Baryshnikov, S. V.; Kuznetsov, B. N.; Cebolla, V. L.; Weber, J. V. Co-pyrolysis of wood biomass and synthetic polymer mixtures. Part I: influence of experimental conditions on the evolution of solids, liquids and gases. *J. Anal. Appl. Pyrolysis* **2002**, *64*, 15−28.

(5) Paradela, F.; Pinto, F.; Gulyurtlu, I.; Cabrita, I.; Lapa, N. Study of the co-pyrolysis of biomass and plastic wastes. *Clean Technol. Environ. Policy* **2009**, *11*, 115−122.

(6) Jesus, M. S.; Napoli, A.; Trugilho, P. F.; Abreu Júnior, Á. A.; Martinez, C. L. M.; Freitas, T. P. Energy and mass balance in the pyrolysis process of Eucalyptus wood. *CERNE* **2018**, *24*, 288−294.

(7) Peterson, A. A.; Vogel, F.; Lachance, R. P.; Fröling, M.; Antal, J. M. J.; Tester, J. W. Thermochemical biofuel production in hydrothermal media: A review of sub- and supercritical water technologies. *Energy Environ. Sci.* **2008**, *1*, 32−65.

(8) Goudnaan, F.; Beld, B.; Boerefijn, F. R.; Bos, G. M.; Naber, J. E.; Wal, S.; Zeevalkink, J. In *Thermal Efficiency of the HTU Process for Biomass Liquefaction*, Fifth International Conference on Progress in Thermochemical Biomass Conversion, 2008; Vol. *18*−*21*, pp 1312−1325.

(9) Xu, C.; Lad, N. Production of heavy oils with high caloric values by direct liquefaction of woody biomass in sub/near-critical water. *Energy Fuels* **2008**, *22*, 635−642.

(10) Demirbas, A. Competitive liquid biofuels from biomass. *Appl. Energy* **2011**, *88*, 17−28.

(11) Bensaid, S.; Conti, R.; Fino, D. Direct liquefaction of lignocellulosic residues for liquid fuel production. *Fuel* **2012**, *94*, 324−332.

(12) Arun, J.; Gopinath, K. P.; SundarRajan, P.; JoselynMonica, M.; Felix, V. Co-liquefaction of Prosopis juliflora with polyolefin waste for production of high grade liquid hydrocarbons. *Bioresour. Technol.* **2019**, *274*, 296−301.

(13) Wang, B.; Huang, Y.; Zhang, J. Hydrothermal liquefaction of lignite, wheat straw and plastic waste in sub-critical water for oil: Product distribution. *J. Anal. Appl. Pyrolysis* **2014**, *110*, 382−389.

(14) Yuan, X.; Cao, H.; Li, H.; Zeng, G.; Tong, J.; Wang, L. Quantitative and qualitative analysis of products formed during co-liquefaction of biomass and synthetic polymer mixtures in sub- and supercritical water. *Fuel Process. Technol.* **2009**, *90*, 428−434.

(15) Sugano, M.; Komatsu, A.; Yamamoto, M.; Kumagai, M.; Shimizu, T.; Hirano, K.; Mashimo, K. Liquefaction process for a hydrothermally treated waste mixture containing plastics. *J. Mater. Cycles Waste Manage.* **2009**, *11*, 27−31.

(16) Wu, X.; Liang, J.; Wu, Y.; Hu, H.; Shaobin, H.; Wu, K. Co-liquefaction of microalgae and polypropylene in sub-/super-critical water. *RSC Adv.* **2017**, *7*, 13768−13776.

(17) Raikova, S.; Knowles, T. D. J.; Allen, M. J.; Chuck, C. J. Co-liquefaction of Macroalgae with Common Marine Plastic Pollutants. *ACS Sustainable Chem. Eng.* **2019**, *7*, 6769−6781.

(18) Coma, M.; Martinez-Hernandez, E.; Abeln, F.; Raikova, S.; Donnelly, J.; Arnot, T.; Allen, M.; Hong, D. D.; Chuck, C. J. Organic waste as a sustainable feedstock for platform chemicals. *Faraday Discuss.* **2017**, *202*, 175−195.
(19) Hongthong, S.; Raikova, S.; Leese, H. S.; Chuck, C. J. Co-processing of common plastics with pistachio hulls via hydrothermal liquefaction. *Waste Manage.* **2020**, *102*, 351−361.
(20) Biller, P.; Ross, A. B. Potential yields and properties of oil from the hydrothermal liquefaction of microalgae with different biochemical content. *Bioresour. Technol.* **2011**, *102*, 215−225.
(21) Akhtar, J.; Kuang, S. K.; Amin, N. S. Liquefaction of empty palm fruit bunch (EPFB) in alkaline hot compressed water. *Renewable Energy* **2010**, *35*, 1220−1227.
(22) Karagöz, S.; Bhaskar, T.; Muto, A.; Sakata, Y.; Oshiki, T.; Kishimoto, T. Low-temperature catalytic hydrothermal treatment of wood biomass: analysis of liquid products. *Chem. Eng. J.* **2005**, *108*, 127−137.
(23) Xu, D.; Lin, G.; Guo, S.; Wang, S.; Guo, Y.; Jing, Z. Catalytic hydrothermal liquefaction of algae and upgrading of biocrude: A critical review. *Renewable Sustainable Energy Rev.* **2018**, *97*, 103−118.
(24) Hirano, Y.; Miyata, Y.; Taniguchi, M.; Funakoshi, N.; Yamazaki, Y.; Ogino, C.; Kita, Y. Fe-assisted hydrothermal liquefaction of cellulose: Effects of hydrogenation catalyst addition on properties of water-soluble fraction. *J. Anal. Appl. Pyrolysis* **2020**, *145*, No. 104719.
(25) Raikova, S.; Smith-Baedorf, H.; Bransgrove, R.; Barlow, O.; Santomauro, F.; Wagner, J. L.; Allen, M. J.; Bryan, C. G.; Sapsford, D.; Chuck, C. J. Assessing hydrothermal liquefaction for the production of bio-oil and enhanced metal recovery from microalgae cultivated on acid mine drainage. *Fuel Process. Technol.* **2016**, *142*, 219−227.
(26) Stefanidis, S. D.; Kalogiannis, K. G.; Iliopoulou, E. F.; Lappas, A. A.; Pilavachi, P. A. In-situ upgrading of biomass pyrolysis vapors: Catalyst screening on a fixed bed reactor. *Bioresour. Technol.* **2011**, *102*, 8261−8267.
(27) Cheng, S.; Wei, L.; Zhao, X.; Julson, J. Application, Deactivation, and Regeneration of Heterogeneous Catalysts in Bio-Oil Upgrading. *Catalysts* **2016**, *6*, No. 195.
(28) Panda, A.; Singh, R. K. Catalytic performances of kaoline and silica alumina in the thermal degradation of polypropylene. *J. Fuel Chem. Technol.* **2011**, *39*, 198−202.
(29) Duan, P.; Savage, P. E. Hydrothermal Liquefaction of a Microalga with Heterogeneous Catalysts. *Ind. Eng. Chem. Res.* **2011**, *50*, 52−61.
(30) Valentini, F.; Kozell, V.; Petrucci, C.; Marrocchi, A.; Gu, Y.; Gelman, D.; Vaccaro, L. Formic acid, a biomass-derived source of energy and hydrogen for biomass upgrading. *Energy Environ. Sci.* **2019**, *12*, 2646−2664.
(31) Matsagar, B. M.; Wang, Z.-Y.; Sakdaronnarong, C.; Chen, S. S.; Tsang, D. C. W.; Wu, K. C.-W. Effect of Solvent, Role of Formic Acid and Rh/C Catalyst for the Efficient Liquefaction of Lignin. *ChemCatChem* **2019**, *11*, 4604−4616.
(32) Biller, P.; Riley, R.; Ross, A. B. Catalytic hydrothermal processing of microalgae: Decomposition and upgrading of lipids. *Bioresour. Technol.* **2011**, *102*, 4841−4848.
(33) Panda, A.; Singh, R. K.; Mishra, D. Thermolysis of waste plastics to liquid fuel: A suitable method for plastic waste management and manufacture of value added products–A world prospective. *Renewable Sustainable Energy Rev.* **2010**, *14*, 233−248.
(34) Wang, K.; Kim, K. H.; Brown, R. C. Catalytic pyrolysis of individual components of lignocellulosic biomass. *Green Chem.* **2014**, *16*, 727−735.
(35) Zhang, X.; Lei, H.; Zhu, L.; Qian, M.; Zhu, X.; Wu, J.; Chen, S. Enhancement of jet fuel range alkanes from co-feeding of lignocellulosic biomass with plastics via tandem catalytic conversions. *Appl. Energy* **2016**, *173*, 418−430.
(36) Zhang, H.; Zheng, J.; Xiao, R.; Shen, D.; Jin, B.; Xiao, G.; Chen, R. Co-catalytic pyrolysis of biomass and waste triglyceride seed oil in a novel fluidized bed reactor to produce olefins and aromatics integrated with self-heating and catalyst regeneration processes. *RSC Adv.* **2013**, *3*, 5769−5774.
(37) Jacobson, K.; Maheria, K. C.; Kumar Dalai, A. Bio-oil valorization: A review. *Renewable Sustainable Energy Rev.* **2013**, *23*, 91−106.
(38) Ye, J.; Cao, Q.; Zhao, Y. Co-pyrolysis of Polypropylene and Biomass. *Energy Sources, Part A* **2008**, 1689−1697.
(39) Ladislav, S.; Kubinec, R.; Jurdáková, H.; Hájeková, E.; Martin, B. GC-MS of polyethylene and polypropylene thermal cracking products. *Pet. Coal* **2006**, 48.
(40) Hájeková, E.; Špodová, L.; Bajus, M.; Mlynková, B. Separation and characterization of products from thermal cracking of individual and mixed polyalkenes. *Chem. Pap.* **2007**, *61*, 262−270.
(41) Chun, Y.; Sheng, G.; Chiou, C. T.; Xing, B. Compositions and Sorptive Properties of Crop Residue-Derived Chars. *Environ. Sci. Technol.* **2004**, *38*, 4649−4655.
(42) Chen, X.; Chen, G.; Chen, L.; Chen, Y.; Lehmann, J.; McBride, M. B.; Hay, A. G. Adsorption of copper and zinc by biochars produced from pyrolysis of hardwood and corn straw in aqueous solution. *Bioresour. Technol.* **2011**, *102*, 8877−8884.
(43) Tan, X.; Liu, Y.; Zeng, G.; Wang, X.; Hu, X.; Gu, Y.; Yang, Z. Application of biochar for the removal of pollutants from aqueous solutions. *Chemosphere* **2015**, *125*, 70−85.
(44) European Commission Publications Office. *General Union Environment Action Programme to 2020: Living Well, within the Limits of Our Planet*; Publications Office of the European Union: Luxembourg, 2014; p 92.
(45) Lee, Y.; Eum, P.-R.-B.; Ryu, C.; Park, Y.-K.; Jung, J.-H.; Hyun, S. Characteristics of biochar produced from slow pyrolysis of Geodae-Uksae 1. *Bioresour. Technol.* **2013**, *130*, 345−350.
(46) Devasahayam, S.; Bhaskar Raju, G.; Mustansar Hussain, C. Utilization and recycling of end of life plastics for sustainable and clean industrial processes including the iron and steel industry. *Mater. Sci. Energy Technol.* **2019**, *2*, 634−646.
(47) Hietala, D. C.; Faeth, J. L.; Savage, P. E. A quantitative kinetic model for the fast and isothermal hydrothermal liquefaction of *Nannochloropsis* sp. *Bioresour. Technol.* **2016**, *214*, 102−111.
(48) Gollakota, A. R. K.; Kishore, N.; Gu, S. A review on hydrothermal liquefaction of biomass. *Renewable Sustainable Energy Rev.* **2018**, *81*, 1378−1392.
(49) Cai, J.; Wang, Y.; Zhou, L.; Huang, Q. Thermogravimetric analysis and kinetics of coal/plastic blends during co-pyrolysis in nitrogen atmosphere. *Fuel Process. Technol.* **2008**, *89*, 21−27.
(50) Ayeni, A. O.; Hymore, F. K.; Mudliar, S. N.; Deshmukh, S. C.; Satpute, D. B.; Omoleye, J. A.; Pandey, R. A. Hydrogen peroxide and lime based oxidative pretreatment of wood waste to enhance enzymatic hydrolysis for a biorefinery: Process parameters optimization using response surface methodology. *Fuel* **2013**, *106*, 187−194.
(51) Cheng, Y.; Zhao, P.-X.; Alma, M. H.; Sun, D.-F.; Li, R.; Jiang, J.-X. Improvement of direct liquefaction of technical alkaline lignin pretreated by alkaline hydrogen peroxide. *J. Anal. Appl. Pyrolysis* **2016**, *122*, 277−281.
(52) Karagöz, P.; Rocha, I.; Özkan, M.; Angelidaki, I. Alkaline peroxide pretreatment of rapeseed straw for enhancing bioethanol production by Same Vessel Saccharification and Co-Fermentation. *Bioresour. Technol.* **2012**, *104*, 349−357.
(53) Huang, H.-j.; Yuan, X.-z.; Zeng, G.-m.; Liu, Y.; Li, H.; Yin, J.; Wang, X.-l. Thermochemical liquefaction of rice husk for bio-oil production with sub- and supercritical ethanol as solvent. *J. Anal. Appl. Pyrolysis* **2013**, *102*, 60−67.
(54) Long, J.; Xu, Y.; Wang, T.; Yuan, Z.; Shu, R.; Zhang, Q.; Ma, L. Efficient base-catalyzed decomposition and in situ hydrogenolysis process for lignin depolymerization and char elimination. *Appl. Energy* **2015**, *141*, 70−79.
(55) Ouyang, X.; Huang, X.; Zhu, Y.; Qiu, X. Ethanol-Enhanced Liquefaction of Lignin with Formic Acid as an in Situ Hydrogen Donor. *Energy Fuels* **2015**, *29*, 5835−5840.


https://dx.doi.org/10.1021/acsomega.0c02854
*ACS Omega* 2020, 5, 20586−20598

(56) Brown, T. M.; Duan, P.; Savage, P. E. Hydrothermal Liquefaction and Gasification of *Nannochloropsis* sp. *Energy Fuels* **2010**, *24*, 3639−3646.
(57) Zhou, D.; Zhang, L.; Zhang, S.; Fu, H.; Chen, J. Hydrothermal Liquefaction of Macroalgae Enteromorpha prolifera to Bio-oil. *Energy Fuels* **2010**, *24*, 4054−4061.



https://dx.doi.org/10.1021/acsomega.0c02854
*ACS Omega* 2020, 5, 20586−20598